Towards an ab-axis giant proximity effect using ionic liquid gating

Atesci, H.

Chapter 2

Ionic Liquids

For their importance in this thesis as a whole, a separate chapter is dedicated to the many aspects of ionic liquid (IL) gating. Gating by means of ILs covers only a small fraction of the total amount of research involving ionic liquids, the total research area of which has relevance in electrochemistry, photo chemistry, catalysis, electronics, and even clean energy [44, 45]. In terms of electrochemical aspects, ILs offer interesting research into memresistive devices. As an example, IL-induced memresistive properties have been shown in WO_x [46], TaO_x [47], TiO_x [48], $SrTiO_3$ [49]and ZnO [50], the crux of which is the ability to attain controllable switching by means of structural or chemical defects. More relevant to the work done in this thesis is the importance of ionic liquid gating in the field of electronics, where the ability to large charge carrier densities is key. In this field, a large amount of research has been done on a host of materials including topological insulators [51], dichalocogenides [52–54], graphene [55], nickelates [56], manganites [57, 58], cuprates [10, 59–66] and other oxides [11, 67–73]. The oxide class of materials is the most relevant to this thesis, and hence the review below is dedicated specifically to ionic liquid gating experiments on these materials. For its importance in this thesis as whole, this chapter is dedicated to a literature discussion on charge carrier density induction using ionic liquids.

2.1 Controlling the surface charge carrier density

ILs are molten salts having melting points below 373 K [44]. ILs are composed of organic or inorganic ions and differ from aqueous electrolytes in the absence of a solvent. Although the first IL was synthesized in 1914 [74], it took a long time before its first application for electrochemical studies, which started in 1980s. Since then, over 10^6 possible ILs have been proposed to exist [75]. The main cations that are used in IL applications are alkyls (C_nH_{2n+1}) bonded to pyridinium (C_5H_5NH), imidazolium ($C_3N_2H_4$), phosphonium (PH_4), ammonium (NH_4), etc. These are combined with anions such as BF_4^-, PF_6^-, NO_3^-, Cl^-, CH_3COO^-, $CF_3SO_3^-$ and $(CF_3SO_2)_2N^-$ [44].

The charged and solvent-free nature of ILs tends to lead to complex molecular organization and structure such as ion pairing or ion aggregation, governed by Coulombic, van der Waals, dipole-dipole interactions, hydrogen-bonding, and solvophobic forces. [76]. Hence, the properties of ILs are too complex to be described by classical theories for aqueous electrolytes [77]. By playing with the ionic species or length of cations and anions, the intrinsic cohesive and repulsive interaction profile of the ions changes, allowing one to change properties such as hydrophobicity, electrical conductivity, viscosity, melting point, and the electrochemical window.

The interfacial physics of ionic liquids is equally complex. In the most simple description, developed in 1853 by Helmholtz [78], two plates are assumed to be connected via an ionic liquid. A potential difference between these plates will drive a layer of cations (anions) to the surface by the electric field of the electrode plane at negative (positive) potential. Due to the fact that an ionic liquid is a good conductor the potential drop in the bulk of the liquid at the end of the process is zero. Screening of the electric field thus needs to happen at the interface with the plates. In short, the interfaces will form charged layers, or so-called electric double layers (EDLs), in essence a nanoscopic version of the macroscopic capacitor. The entire potential drop happens between these charged layers. The potential drop depends on the choice of model and the level of approximation, but in Fig. 2.1a we assume the profile to be linear.

In standard oxide dielectric field effect transistors (FETs), the drop in the potential happens over a distance which is up to two

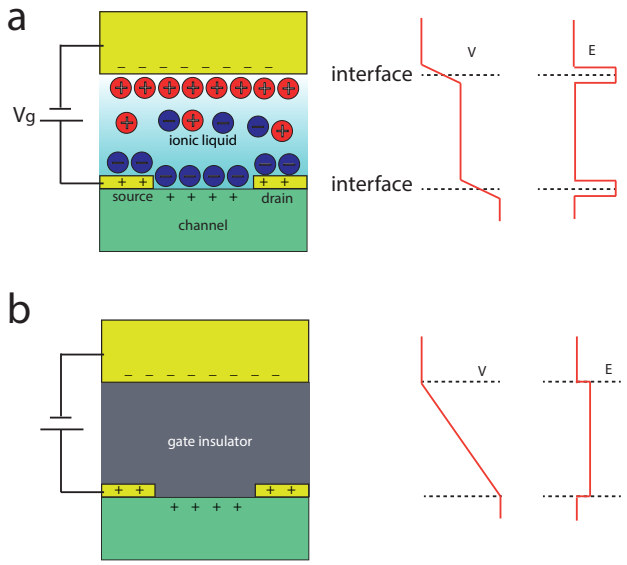

Figure 2.1: **(a)** Schematic overview of the gate/IL/channel system. A gate voltage V_g is applied between gate and source and the electric field is screened at the electrode and channel interfaces with EDLs. The potential difference V is maximized at the interfaces, approximated as a linear functions, with no potential difference in the IL. The electric field E, therefore, is maximized at the EDLs. **(b)** In a standard oxide dielectric field effect transistor, the drop in potential is distributed over distances that are up to two orders of magnitude larger than the EDL separation distance, leading to a substantially limited induced electric field.

orders of magnitude larger than in the case of EDLs (Fig. 2.1b) [79]. The induced polarization σ at a gate voltage V_g across a dielectric of thickness d and dielectric constant ϵ_r follows from Coloumb′s law as $\sigma = \epsilon_0 \epsilon_r V_g/d$. Hence, the implications of a larger thickness to the induced polarization can, in principle, be compensated by applying a larger gate voltage. However, oxides tend to break down when a very high electric field E is applied across them, such that V_g has to be kept below $E_b d$, with E_b the breakdown field. The much-used SiO_2 in conventional Si FETs, for example, has a breakdown field of 10 MV/cm [80]. Together with a dielectric constant of $\epsilon_r = 3.9$, this leads to maximum polarization of 3.5 μC/cm^2 (or 2×10^{13} charges/cm^2), which is relatively small compared to polarization levels attainable with ionic liquids, typically in the order of $10 - 100$ μC/cm^2 [80].

The penetration of the electric field into a conducting film is counteracted by electrostatic screening, essentially limiting the field effect. The amount of screening depends on a variety of factors, as is formulated by the Thomas-Fermi model: the electric field in the conductor decays exponentially with a decay constant λ_{TF}. In the high-T_c cuprate superconductor $La_{2-x}Sr_xCuO_4$, $n_0 \sim 1.6\times 10^{21}$/cm^3 at optimal doping $x = 0.15$, while ϵ_r is about 30 [81], resulting in a screening length of approximately 11 Å, i.e. slightly less than the c-axis lattice parameter of the unit cell. The superconducting properties at the surface are only fully tunable by the external, transverse electric field when λ_{TF} dominates the coherence length in the same direction, ξ_z. In the case of $La_{2-x}Sr_xCuO_4$, ξ_z is 2.2 Å [82], which is sufficiently small.

The field-induced surface charge carrier density induced by the IL gating can be written as [83]

$$\Delta n = \frac{1}{d}\int_0^d \frac{\epsilon_0 \epsilon_{\mathrm{IL}} E}{e\lambda_{\mathrm{TF}}} e^{-z/\lambda_{\mathrm{TF}}} dz = \frac{\epsilon_0 \epsilon_{\mathrm{IL}} E}{ed}(1 - e^{-d/\lambda_{\mathrm{TF}}}). \tag{2.1}$$

Here, e is the electron charge, while ϵ_{IL} is the dielectric constant of the IL of 14.5 [84] of, in this case, N,N-diethyl-N-(2-methoxyethyl)-N-methylammonium bis(trifluoromethylsulfonyl)imide (DEME-TFSI). Furthermore, d is the EDL distance of typically 1 nm. Assuming $d \gg \lambda_{\mathrm{TF}}$, the equation simplifies to $\Delta n = \frac{\epsilon_0 \epsilon_{\mathrm{IL}} E}{ed}$. Hence, to turn the surface layer of the material of interest, the cuprate Mott-insulator La_2CuO_4 into its optimally doped state, a gate voltage of -2.0 V is needed.

In the experimental literature of $La_{2-x}Sr_xCuO_4$, we find that the effect is achieved at $V_g = -4.5$ V for the same IL and active film thickness, i.e. 1 UC [10]. For other materials, even smaller charge carrier densities have been reported. For $La_{0.8}Sr_{0.2}MnO_3$ [57], $SrIrO_4$ [85] and VO_2 [69], it has been found that gating hardly produces any effect electrostatically. These findings indicate that there are some factors that cause some degree of deviation from the ideal Helmholtz scenario, and that the complete process of gating is far from understood.

2.2 Deviations from the ideal Helmholtz scenario

The microstructure and capacitance of the electrical double layers (EDLs) at the IL/electrode interface play an essential role in determining IL-induced transport phenomena in oxides. To gain a certain degree of apprehension of these phenomena, a more detailed picture of the ionic liquid/oxide interface is needed, as there are some factors that contribute to the non-ideal Helmholtz scenarios. Although some experiments suggest that the IL/electrode interface is one ion layer thick (typically 3 to 5 Å) [86], the ideal Helmholtz layer picture negates the role of entropy. Thermal disorder leads to a diffuse EDL, where not all counterions are gathered in one layer [87]. Others have shown that alternating layers of cations and anions are formed and that the layering persists for many monolayers, as has been experimentally verified using X-ray reflectivity techniques [88]. As molecular shapes are often complex, with charges typically delocalized among many atoms, the layering and diffusivity and hence the capacitance of the EDL will also be dependent on these factors. The size of the anions and cations further influence the capacitance, as this will change the spacing between the charged double layers. A smaller ion size, for example results in a larger EDL capacitance, capable of inducing a higher interfacial charge carrier density.

Randomness of the charge order in the ionic liquid at the interface gives rise to a rapidly varying electrostatic potential which results in an exceptionally large decrease in mobility of the charge carriers in materials that are known to have highly mobile charge carrier densities, as experiments done by Petach *et al.* in Ref.89 have shown. In compensation for this effect, some have used a separator layer such

as hexagonal boron nitride to limit the effects of the Coulomb scattering on the mobility [71]. However, the increased electric double layer distance has a negative influence on the polarization. Hence, one can expect an optimum in the induced conductivity as a function of separator layer thickness for gated materials in general, depending on the cation/anion species and the homogeneity of the anion/cation layer [90]. Theoretical studies have shown similar conclusions of inhomogeneity induced by IL in two-dimensional electronic systems based on specific features of the resistivity versus temperature [91], such as the width of the superconducting transition. Inhomogeneity in doping can also be caused by the suboptimal crystallinity and roughness of the surface. It was shown in Ref.92 that FeSe interfaces containing pits, the pits served as electron traps when gated with an IL.

The packing density is another intrinsic property of the EDL which has to be considered. This quantity is influenced by the intrinsic electron structure of the anion or cation. For example, ILs with coordinating imidazolium cations 1-ethyl-3-methylimidazolium ($EMIM^+$) and 1-hexyl-3-methylimidazolium ($HMIM^+$) are delocalized π-electron systems, which tend to have stabilizing stacking interaction between themselves, leading to a denser packing of the cations at the surface [93, 94]. Noncoordinating ammonium-based cations such as N,N-diethyl-N-(2-methoxyethyl)-N-methylammonium ($DEME^+$) do not have a delocalized π-electron imidazolium ring, leading to lower packing densities. The capacitance of the EDL is further dependent on the cation polarizability, and the preferred cation or anion orientation under the applied electric field [44, 86], for this determines the double layer thickness.

2.2.1 Surface electrochemistry

Since the start of IL gating for FET purposes in 1955 [95], there has been a massive amount of research in this field, with the number of published articles on this subject in the order of 10^4, and the number of gated materials in the order of 10^2. However, there seems to be no single, universal IL gating mechanism that applies to all of them [96], and only a fraction of those materials are behaving purely electrostatically when gated. The rest of the materials show some kind of electrochemical behavior.

But how do we distinguish electrochemical processes from electrostatic ones in the context of IL gating of oxides? Many electrochemical

processes like oxygen vacancy production or ion intercalation are characterized by a large pseudocapacitance [97], which, through Faradeic charge transfer processes, accumulates charges in a slow way. Hence, such processes typically have large time constants [98], often leading to hysteresis effects [99]. However, a process with a long time constant is not a unique characteristic for electrochemistry, as there are some electrostatic cases where the interaction between the large electric field in the EDL and the oxygen electric dipole moments in cuprates such as $YBa_2Cu_3O_{7-\delta}$ [100] and $La_{2-x}Sr_xCuO_{4+\delta}$ [64] leads to a rearrangement of oxygen vacancies. In turn, this causes a change in the doping of the CuO_2 planes over time scales of minutes [83], comparable to typical electrostatic processes of hydrogenation and oxygen vacancy production [62, 63, 67]. Other characteristics of electrochemical reactions include irreversibility [101] and irreproducibility [52], though there are some oxygen vacancy processes in VO_2, TiO_2 and $SrTiO_3$ that are known to be reversible and reproducible as well [99].

In other words, electrochemical gating is not always distinguishable from electrostatic gating by means of reversibility, reproducibility and time scales. Although these criteria can still be used, additional measures need to be taken to obtain a complete picture. As charge transfer processes tend to be activated by the gate voltage and temperature, one can turn to the cyclic voltammetry as a tool to distinguish electrochemistry from electrostatics. Any charge transfer process increases the current between the gate and oxide electrodes, leading to a so-called charge transfer peak at the oxidation or reduction potential of the reaction. In case of electrostatics, no peaks are to be expected, and the integrated current should scale as a function of the applied gate voltage, V_g as $Q = CV_g$, with C the capacitance of the EDL interface with the oxide channel. In terms of temperature, the rate of activated processes scales exponentially via $I \propto e^{-E_a/k_BT}$, with I, k_B, T and E_a the current of the activated process, Boltzmann constant, temperature, and activation energy, respectively. The integrated gate current in such a case should follow an exponential behavior as a function of temperature as well.

What factors induce electrochemistry on the surface? If we start with ideal circumstances, the oxide channel is impermeable to ions, and the charge carrier accumulation or depletion happens electrostatically (see Fig. 2.2a). There are factors, however, that promote permeation of ion species to and from the oxide in the form of electron

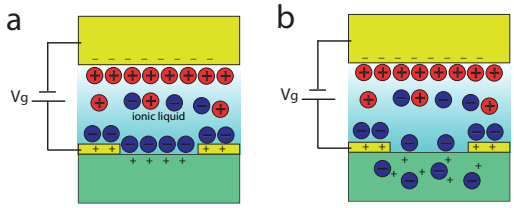

Figure 2.2: **(a)** IL-induced electrostatic gating: the charged interfaces are formed while no ion intercalation takes place, neither are there other processes that lead to stoichiometric changes in the channel. **(b)** In the electrochemical case, the stoichiometry of the channel is changed, in this case by means of ion intercalation.

transfer processes or diffusion of electroactive species (see Fig. 2.2b) [44]. These factors are the chemical affinity of the IL and the oxide surface, the crystal structure and crystalline quality of the oxide, the size and charge of the ions in the IL, or the magnitude and direction of the electric field induced in the EDL, the presence of impurities, the density of step-edges, etc. All of the different factors that could influence the electrochemistry are considered below.

2.2.2 Gate voltage and gate temperature related factors

Electric field-induced electrochemical processes can be independent of the IL-specific electrochemical window (EW) of the ionic liquid, defined as the voltage range in which the ionic liquid neither oxidizes or is reduced, i.e. stays electrochemically inert. The EW is determined by the range of potential differences for which the cation (anion) resists reduction (oxidation), with typical EWs ranging from 2.0-6.0 V at room temperature. Depending on the composition and structure of the ionic liquid and oxide material, there exists a voltage threshold above which electron transfer takes place between the surface and the ions in the liquid. The charge transfer leads to ion diffusion, because the ions converted at the interface need to be replaced, either from the liquid or solid side. The authors of Ref.49 show a bias dependence of oxygen vacancy production in $SrTiO_3$, whereby irreversible oxygen vacancy production is induced at $V_g \geq 3.75$ V, leading to surface degradation of several micrometers deep. Irreversible changes were also seen in nickelates, such as $NdNiO_3$ at $V_g \leq -2.5$ V [56]. For

$YaBa_2Cu_3O_{7-\delta}$, gate voltages as small as 0.9 V [63] or 1.0 V [102] can lead to electrochemical effects related to a change of the oxygen content of the film. Furthermore, electrochemical reactions often are found at only one voltage polarity [103–106]. As an example, $NdNiO_3$ as reported by Ref.107 shows electrochemical reactions for a specific regime of positive gate voltages, while for negative gate voltages no electrochemistry is observed.

When the gating is performed at a relatively high temperature, electrochemistry is induced at a larger rate, even at modest gate voltages. For example, gating experiments on $La_{1/3}Sr_{2/3}FeO_3$ leads to irreversible chemical reactions involving Fe and La migration into the IL, even before applying any gate potential [108]. The authors attribute the observed exchange of ions at the interface to the high gating temperature, related to the melting point of 60 C and to a higher reactivity of the IL used.

The fact that electrochemical processes are activated can be exploited to avoid breakdown at V_g above the EW. Hence, decreasing the temperature reduces the rate of the electrochemical reaction and hence effectively widens the EW. As an example, an EW of 2.7 V is found at room temperature for the IL gating of ZnO with DEME-TFSI [109]. The electrochemical window could be expanded up to 6.0 V simply by reducing the gating temperature to 220 K.

Furthermore, the direction of the field (i.e. polarity of the gate voltage) influences which type of anions or cations are taking place in the reaction. For positive gate voltages, oxygen vacancies can be induced, or cations (e.g. H^+) can be intercalated [69, 96, 102], which is not possible for negative voltages because of the Coulombic repulsive action. For negative gate voltages, oxygenation [63] can be induced, or negative ions can be intercalated [108].

In nickelates, for example, hydroxide ions produced by water electrolysis can react with Ni and degrade the film, as has been shown for $LaNiO_3$ [110]. Similar effects of degradation were observed in $SmNiO_3$ with experiments performed with unbaked IL having water contamination [103]. Furthermore, irreversible behavior is found at other materials, such as the ferromagnetic semiconductor $La_{0.8}Ca_{0.2}MnO_3$ at $V_g = -3$ V due to water contamination of the IL. Other examples include oxygen vacancy production at positive gate voltages in some materials, e.g. $La_{0.8}Sr_{0.2}MnO_3$ [57]. In other cases, e.g. Sr_2IrO_4, it can lead to oxygenation at negative voltages by means of a hydroxila-

tion reaction, i.e. $Sr_2IrO_x + 2\delta OH^- \longrightarrow SrIrO_{x+\delta} + \delta H_2O + 2\delta e^-$ [85].

2.2.3 IL-related factors

IL gating on oxides adds an additional complication in the layering of the EDL, related to the binding affinity of the ions to the oxide surface. It is known that some cations or anions have acidic groups, and the acidic H atom of the imidazolium ring, for example, has a relatively strong coordinative hydrogen bond with the O atoms of an oxide surface, as is the case with TiO_2 [99]. The chemical bonding with the surface tends to be reversible, and increases the packing density and therefore increases the charge carrier density. However, these properties often lead to hysteresis effects and chemical modification [50]. Therefore, noncoordinating cations and an absence of acidic groups in cations is preferred when gating oxides, which is true for $DEME^+$. Similarly, in Ref.111 it was found that replacing the acidic H-atom of the imidazolium cation increases the stability of ZnO devices in ambient conditions. In $La_{1/3}Sr_{2/3}FeO_3$ an intermixing region even without bias application across the EMIM-PF_6/oxide interface leads to a surface reaction with the IL and involving Fe and La cations. This might be caused by the PF_6^- anion reactivity with the surface, or the intrinsic instability of $La_{1/3}Sr_{2/3}FeO_3$ to ionic interfaces.

2.2.4 Packing-related factors

Apart from the properties of the IL, other factors that influence the chemical activity of the oxide surface with the IL is the surface energy of the crystalline facet facing the IL. As an example, it has been shown in TiO_2 that the facets with the highest surface energy tend to form more oxygen vacancies, which act as n-type dopants, and hence lead to a higher charge carrier density. This might be of relevance for gating on $SrTiO_3$, as TiO_2 is one of the terminations of the unit cell, and IL induced oxygen vacancy formation is also reported for this material.

The crystal structure of the oxide electrode interface is equally important influencing the doping mechanism of gating. Oxides with open unit cell structures with a high ionic mobility of oxygen and tendency to form oxygen vacancies, such as VO_2 [67] and $SrTiO_3$ [49], are prime examples of oxides susceptible to oxygen electromigration. Other oxides are relatively stable against oxygen vacancies, but have vacant sites in their unit cells. If these are surrounded by negatively

charged ions, such as O^{2-}, these materials would have the tendency to be more sensitive to H^+ ion intercalation, such as the case with WO_3. And since H^+ is a ubiquitous impurity ion, this kind of electrochemistry would be easily detectible in materials that are prone to cation intercalation [96]. Other forms of intercalation are also possible in such materials involving K^+ and Na^+, for example when using a polyethylene oxide/$KClO_4$ [112] or polyethylene glycol/NaF [113] mixtures, respectively. Other oxides that have more compact crystal structures[113] are not sensitive to intercalation or oxygen electromigration, and hence perform purely electrostatically when gated with ILs, an example of which is indium tin oxide. Similarly, it was found that the high chemical stability of the ferromagnetic semiconductor $Ti_{0.9}Co_{0.1}O_2$ prevented the films from degrading, even at gate voltages of up to 3.8 V [114].

While the above applies for bulk samples, IL gating of thin films is accompanied by extra complications. The lattice mismatch between the film and substrate and other growth conditions can lead to crystalline defects such as grain boundaries and this has been shown to affect the mechanism of gating. As an example, thin films of epitaxially grown VO_2 on TiO_2 show reversible gating, while those grown on the lattice mismatched hexagonal Al_2O_3 lead to irreversible electrochemical reactions when gated [115]. Stoichiometry can also play a role, as is known from Ref.116 for the spinel $Zn_xFe_{3-x}O_4$ as the mechanism of gating changed depending on the Zn doping. The appendix provides the reader with a more comprehensive overview of the IL gating experiments.

2.2.5 Water as electroactive species

Water absorption in ILs is a key issue in IL gating, as it can reduce the EW and alter the device performance through electrochemistry [50, 62]. The presence of water dopes the IL with a weak Brønsted acid, because of which the IL becomes protic. This is accompanied by the formation of a proton and a hydroxyl ion, i.e. H^+ and OH^-. Compared to the typically large organic ions present in an IL, these dissociation products are smaller in size. Hence, at a given gate potential, one of the two species forms a physisorbed inner Helmholtz layer for which the separation distance with the interface is smaller as well, leading to significantly higher electrostatically accumulated charge carrier densities.

As our field of interest involves correlated oxide materials, the electrostatic picture of physisorption is susceptible to change, especially when using a multitude of (correlated) oxide materials having charged atomic layers in the unit cell. Stacking different oxide materials can lead to polar build-up of the electric field, the best example of which is $LaAlO_3$ on TiO_2-terminated $SrTiO_3$ [117]. The polarized termination in oxides, which is accompanied by a large surface energy, makes the surface more sensitive to charged ions [118], even more so to electroactive species such as H^+ or OH^-. When a certain termination has a higher affinity to one of the two species, applying the correct polarity of the gate voltage can lead to a charge transfer processes of hydroxilation or hydrogenation, representing OH^- or H^+ surface chemisorption, respectively. In such scenario, the electron transfer from and to the drain electrode dominates the induced changes in conductivity of the material, as opposed to the electrostatic effect of the EDL, as has been shown for different ZnO surface terminations [50].

More generally, the electroactive nature of H_2O shifts the cathodic (anodic) limiting potential of the sample towards the positive (negative) potential [119], essentially limiting the electrochemical window (EW) of the IL. The shift in the potential depends on the concentration of water in the IL. It has been shown, for example, that a 3 %wt H_2O contamination can diminish the EW by as much as 2.0 V [120]. Effects of unwanted electroactivity have been shown to exist even down to a level of tens of ppm [119]. In the cuprate class of materials relevant for this thesis, it was found in Ref.60 that simply applying the IL (DEME-TFSI) on the channel of a $LaCuO_{4+\delta}$ film even before applying any gate potential leads to the reduction of its conductivity and T_c of close to 20 K. Similar effects were found at the moment of application of the IL on a $YBa_2Cu_3O_{7-\delta}$ channel[62]. This is likely due to damage by the water contained in the liquid, as pumping eliminated the decrease in conduction.

Ionic liquids are also expected to have traces of halides, acids, residual solvents and other residuals which originate from the fabrication process, which, in principle, can act as dopants of the IL, similar to water. Likewise, similar electrochemical effects could be expected of these dopants if present in sufficiently large concentrations.

2.3 Conclusions

Ideally, we would like the electrochemical component of IL gating to be minimized, as some of the electrochemistry is irreversible and can affect the experiments in a negative way.

For this, we prefer the noncoordinating $DEME^+$ ion as this has a weak bond with oxygen atoms of the oxide material, as discussed in Section 2.2.

Furthermore, the IL should be kept free from any water as much as possible, as this is an electroactive species. One way of achieving this requirement is by selecting a hydrophobic IL [119], for example those with a bis(trifluoromethylsulfonyl)imide (TFSI) cation [121], widely used in IL gating experiments [8, 10, 49, 98, 122]. Furthermore, the partial pressure of these molecules has to be minimized. The reader is referred to Section 3.6 for a more specific description of the IL treatment.

Other considerations include the temperature, which has to be kept as low as possible while charging the ionic liquid, as the activated processes of electrochemistry are exponentially dependent on the temperature, as discussed in Section 2.2.2. Hence, to effectively maximize the EW, the experimental gate temperature needs to be minimized. To facilitate this, an IL needs to be chosen with a minimal melting temperature. DEME-TFSI has one of the lowest melting temperatures available for ILs of 183 K. Hence, together with the previous considerations in mind, we have decided to use DEME-TFSI for the IL gating experiments presented in this thesis.

2.4 Appendix

Here, the IL gating mechanism on a number of oxide materials, along with some its key parameters, are listed.

Material	IL	Gate (K) Temp.	IL treatment	V_g range	Gating mechanism	Ref.
Ferromagnetic semiconductors						
$La_{0.7}Sr_{0.3}MnO_3$	P(VDF-TrFE)	300	-	-35V$\leq V_g \leq$ 35V	EC (oxygen vacancy)	[123]
$Pr_{0.65}(Ca_{0.75}Sr_{0.25})_{0.35}MnO_3$	DEME-TFSI	230	-	-3$\leq V_g \leq$ 3V	ES	[124]
$Ca_{1-x}Ce_xMnO_3$	DEME-TFSI	300	1 Torr	0$\leq V_g \leq$ 2V	ES	[125]
$La_{0.525}Pr_{0.1}Ca_{0.375}MnO_3$	DEME-TFSI	220	-	-3V$\leq V_g \leq$ 3V	ES for -2V$\leq V_g \leq$ 2V EC for $\lvert V_g \rvert \geq$ 2V	[126]
$Ti_{0.9}Co_{0.1}TiO_3$	DEME-TFSI	300-320	-	0$\leq V_g \leq$ 3.8V	ES	[114]
$La_{0.8}Ca_{0.2}MnO_3$	EMIM-TFSI/ polyethylyne oxide + $LiClO_4$	298	-	-3$\leq V_g \leq$ 3V	EC for Vg = 3V	[127]
Ferrates						
$Zn_xFe_{3-x}O_4$	DEME-TFSI	300	5×10^{-5}Torr	-1.5$\leq V_g \leq$ 1.5V	EC (oxygen vacancy)	[116]
$La_{1/3}Sr_{2/3}FeO_3$	EMI-PF6	333K	-	-2$\leq V_g \leq$ 0V	EC:La/Fe migration	[108]
Nickelates						
$SmNiO_3$	TMEM-Py4	220	N_2 atmosphere	-2.5$\leq V_g \leq$ 0V	Without IL treatment: electrochemical etching for $V_g \leq$-1.2V With IL treatment: ES for -2.5$g \leq$0V EC for $V_g \geq$0V	[103]
$NdNiO_3$	BMPyr-TFSI	280	p_{O_2,H_2O} $\leq$ 1 ppm	-4V$\leq V_g \leq$ 0V	ES for -3$\leq V_g \leq$ 0V EC for $V_g \leq -4V$ or $V_g \geq$ 0V	[104]
$NdNiO_3$	EMIM-DCA	240	120 C for 48 h	-2.5V$\leq V_g \leq$ 2.5V	EC for $V_g \geq$ 0V: oxygen vac. ES for $V_g \leq$ 0V	[105]
$SmNiO_3$	TMEM-Py4	433	160C for 12h	-2V$\leq V_g \leq$ 2V	EC for $V_g \leq$ 0V:oxygenation $V_g \geq$ 0V:oxygen vacancy	[106]

Material	IL	Gate (K) Temp.	IL treatment	V_g range	Gating mechanism	Ref.
Titanates						
$SrTiO_3$	PS-PMMA-PS:EMI-TFSI	300	-	$2.8V \leq V_g \leq 3.5V$	-	[73]
$SrTiO_3$	DEME-TFSI	190-210	10^{-5} Torr	$0V \leq V_g \leq 3V$	ES	[128]
$SrTiO_3$	EMIM-TFSI	300	10^{-7} mbar, 120 C for 12 h,	$0V \leq V_g \leq 2V$	EC: oxygen vacancy	[70]
$SrTiO_3$	Polyethylene oxide+$KClO_4$	320	-	$2V \leq V_g \leq 5V$	ES for $V_g \leq 3.75V$ EC:$V_g \geq 3.75V$	[49]
TiO_2	DEME/EMIM/HMIM-TFSI	280	10^{-7} Torr, 120 C for 12 h	$-2.3V \leq V_g \leq 2.3V$	EC: oxygen vacancy	[99]
Cuprates $La_2CuO_{4+\delta}$	DEME-TFSI	240	-	$1.2V \leq V_g \leq 3.0V$	EC	[60]
$La_{2-x}Sr_xCuO_4$	EMIM-DCA	300	-	$-2.5V \leq V_g \leq 3.2V$	ES: oxygen displacement	[64]
$YBa_2Cu_3O_{7-\delta}$	DEME-TFSI	220	10^{-2}Torr	$-4V \leq V_g \leq 10V$	EC: oxygen migration	[63]
$YBa_2Cu_3O_{7-\delta}$	Polyethylyne oxide+$KClO_4$	300	-	$0V \leq V_g \leq 3V$	EC for $V_g \geq 1V$	[102]
$YBa_2Cu_3O_{7-\delta}$	DEME-TFSI	240	-	$-2.52V \leq V_g \leq 2.0V$	inconclusive	[129]
$YBa_2Cu_3O_{7-\delta}$	Polyethylyne oxide+$KClO_4$/ Polyethylyne oxide+$CsClO_4$	300	-	$0V \leq V_g \leq 3V$	EC for $V_g \geq 0$V:oxygen vacancy	[130]
$Nd_{2-x}Ce_xCuO_{4-\delta}$	DEME-TFSI	210	60 C for several days	$0V \leq V_g \leq 2.5V$	EC	[131]

Material	IL	Gate (K) Temp.	IL treatment	V_g range	Gating mechanism	Ref.
Other oxides						
$SmCoO_3$	DEME-BF4	300	-	-2V$\leq V_g \leq$ 0V	ES	[132]
ZnO	DEME-TFSI	220	10^{-1}Torr	0V$\leq V_g \leq$ 6V	ES	[109]
ZnO	EMIM-TFSI,EMIM-TCB, EMIM-FAP,HMIM-FAP, EMMIM-TFSI,BMMIM-TFSI BMIM-TFSI	300	10^{-2}mbar, 60 C for 12 h	1.5V$\leq V_g \leq$ 1.5V	ES except for BMIM-TFSI EC in ambient air	[111]
WO_3	DEME-TFSI, polyethylyne glycol+NaF	294-304	10^{-6}Torr	-2V$\leq V_g \leq$ 2V	EC:hydrogen intercalation	[96]
WO_3	DEME-TFSI	230	120 C for several days	0V$\leq V_g \leq$ 2V	ES	[133]
WO_3	DEME-TFSI, polyethylyne oxide+$LiClO_4$	300	70 C for several days	-2V$\leq V_g \leq$ 2V	ES for DEME-TFSI, EC (Li^+ intercalation) for polyethylyne oxide+$LiClO_4$	[134]
WO_3	EMIM-TFSI,PYR14-TFSI	300	10^{-6} Torr, 80 C overnight	-1.5V$\leq V_g \leq$ 1.5V	EC: protonation	[97]
Indium-tin-oxide	DEME-TFSI	-	-	0$\leq V_g \leq$ 2.5V	ES	[113]
InO_x	EMIM-TFSI	300	$p_{O_2,H_2O} \leq 5000ppm$	-1.03V$\leq V_g \leq$ 1.03V	-	[135]
VO_2	DEME-TFSI	-	-	-3V$\leq V_g \leq$ 3V	ES	[11]
VO_2	HMIM-TFSI	300	-	-3V$\leq V_g \leq$ 3V	EC for $V_g \geq$ 1.5V: oxygen vacancy	[67]
$SrRuO_3$	EMI-TFSI	300	10^{-6} Torr	-2.5V$\leq V_g \leq$ 3V	EC:oxygen vacancy	[136]